2024 COSMIC Capstone Challenge

Orbital Catch & Release

Tri-State Horizon

Wesley Green[1], Brandon Gero[1], Braden Johnson[1], Ashley Loftis[1], Rachael Krugh[1], Lyze Glenister[1], Brian Holt[2], and Sara Lego[3]

April 8, 2024

Abstract

This mission demonstrates the capture and release of in-orbit space debris using a payload integrated with the BCT X-Sat Venus Class Bus. The demonstration targets the Electron Kick Stage R/B (ID #60420) and utilizes a capture approach consisting of soft-capture via robotic arms equipped with gecko gripper end-effectors and hard-capture via a multi-pin pressure sensor chamber. The spacecraft maneuvers to rendezvous with the debris, confirming orientation before executing capture operations. The gecko grippers enable secure, damage-free attachment, while the pressure sensor chamber molds around the debris, allowing for stable containment and transport. Following mission progression to the predetermined orbit, a controlled release ensures the debris remains on its intended trajectory without added velocity. The payload design incorporates a foldable robotic arm system, gecko gripper end-effectors, and an adaptive multi-pin chamber, each optimized for handling irregularly shaped debris. This mission serves as a crucial step in advancing space debris removal methodologies, enhancing orbital sustainability, and mitigating collision risks for future operations.

1 Introduction

In-Space Servicing, Assembly, and Manufacturing (ISAM) is the next big step in the development of space technologies and capabilities. However, there is a large capability gap between where we are now with the technology and where we need to be to reach our long-term goals of conducting ISAM missions [1]. The background research that was conducted for this mission played an important role in the design concepts that were developed. To begin, general research was conducted on ISAM where information was collected on the current efforts and technological developments, as well as on current satellites and space debris in orbit [2]. It was

[1] Pennsylvania State University Undergraduate Student in Aerospace Engineering. For further author correspondence: Ashley Loftis acl5736@psu.edu
[2] Industry Mentor. For further mentor correspondence: Brian Holt brian.holt@exotrail-us.com
[3] Pennsylvania State University Aerospace Engineering Faculty Advisor

from this initial research that the decision to develop a payload that could dispose of in-orbit space debris was made. This payload will help bridge the gap between current and future technology focused on removing space debris. This payload can be used to decrease the likelihood of collisions which will reduce risks for future missions.

Further exploration delved into the characteristics of space debris, such as average size and weight, and examined potential methods for capturing and securing debris. Research efforts included studying robotic arms, considering options like the Canadarm [3] and pneumatic and inflatable arms [4]. Additionally, various attachment mechanisms for securing debris were analyzed, including magnets [5], gecko grippers [6], and pressure chambers [7]. These investigations provided critical insights into how different robotic arms and attachment strategies could be employed to achieve the mission's objectives effectively.

2 Mission Overview

This mission demonstrates the capture and release of chosen space debris. Three concepts were developed based upon the research done to determine capture and release mechanisms. After a concept trade study was conducted, it was determined that the capture procedure will include a soft-capture, using robotic arms and gecko gripper end-effectors, and a hard-capture, which is a multipin pressure sensor chamber. Once the debris is captured inside the chamber, the arms are stored, and the debris can be transported. After transportation, the release procedure will begin, and everything will be undone to release the debris from the payload's grasp.

The top-level objectives were developed based on the selected capability gap, mission operations, and payload integration constraints with the BCT X-Sat Venus Class Bus. Because of the limitations of our payload size, the debris that is chosen will also be held to those limitations. With that, the team decided that the debris will have to be within $136 - 227\ kg$ and between $0.5 - 1.5\ m$. For both capture and release, the debris should not be damaged during the capability demonstrations. During the release portion of the demonstration, there should not be any extra velocity added to the released debris so that it stays on track to its destination. For the integration with the bus, the payload is given the following specific constraints highlighted in the RFP: survivability in the LEO environment, maximum volume of 17" x 16.4" x 27", maximum mass of 70 kg, and require less than 444 W of power.

Using the top-level objectives and mission operations, mechanisms were selected for each subsystem to ensure mission success. With each mechanism selected, a mass budget and power budget were developed. The mass budget is displayed in Table 1, with the needed mass shown for each system and subsystem and a total reserve of 7 kg or 10%.

Table 1 Mass Budget

System	Subsystem	Component	Mass (kg)	Percentage
BCT X-Sat Venus Class Bus	Communication	Patch Antenna	0.075	0.11%
	Power	6x Batteries	8.15	11.65%
	GNC	FlexCore, 4x RW8, 2 NST	17.0	24.30%

	C&DH	Computer	5.0	7.15%
	Propulsion	Orbion Aurora Thrusters	14.5	20.72%
	Thermal	Thermistors	Negligible	0%
	Reserve	-	3.5	5%
		Total:	48.225	68.92%
Payload	C&DH	Transceiver and Computer	5.19	7.42%
	Structure	Primary Structure, Gecko Grippers, Robotic Arms, Pressure Chamber & Sensors	10.88	15.55%
	Thermal	Heater and Thermistors	0.175	0.25%
	Optical Tracking	Obruta RPOD Kit	2.0	2.86%
	Reserve	-	3.5	5%
		Total:	21.745	31.08%
		Total Mass:	69.97	100%

The power budget is displayed in Table 2, with the total power required by each system and subsystem and a reserve of 403.17 W or 30%. The payload was designed to only use 444 W from the host spacecraft and has extra batteries to offset the provided power with the needed power.

Table 2 Power Budget

Subsystem	Average Nominal Voltage (V-DC)	Total Peak Wattage (W)
Communication	28	22.75
C&DH	12	12.60
Propulsion + AOCS	28	840.0
Thermal	12	45.08
Optical Tracking	12	20.3
Reserve	-	403.17
Total Peak Power:	1343.9 W	

2.1 Macro-level Mission Architecture

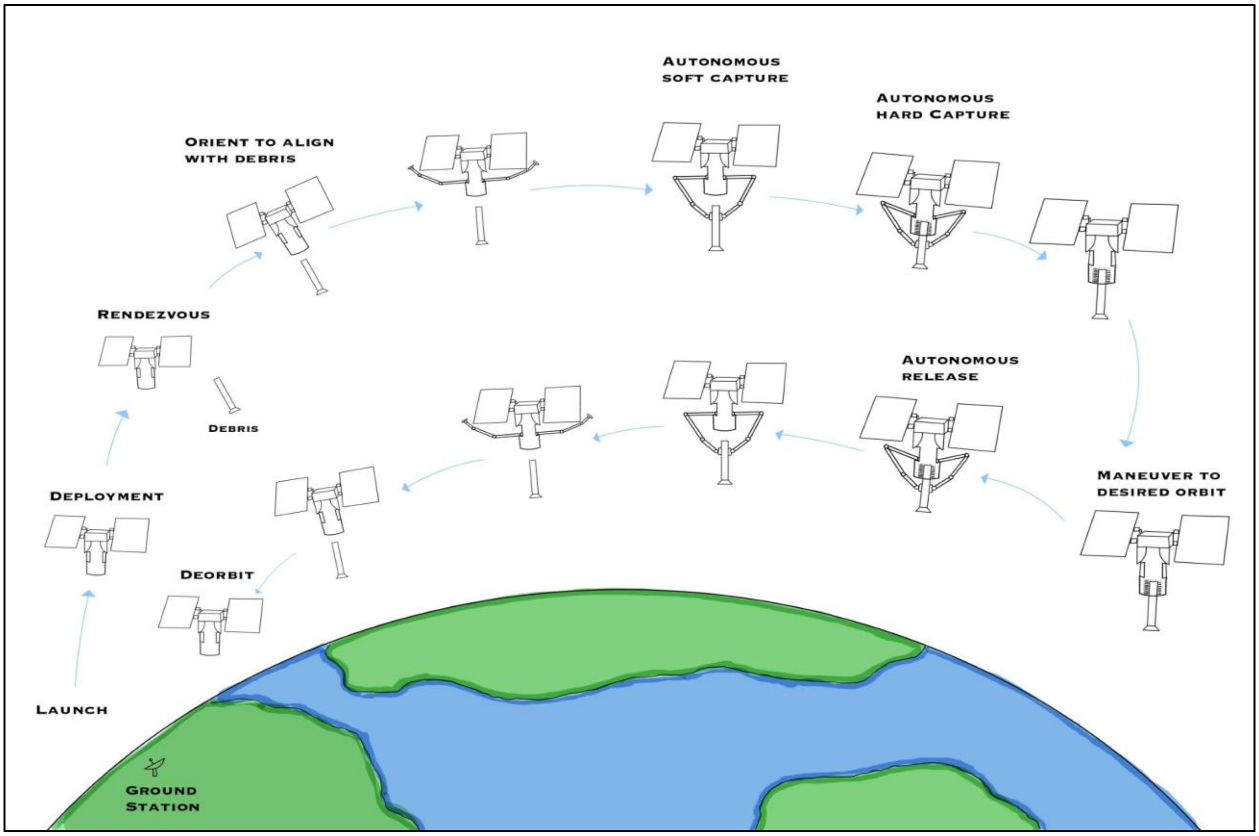

Figure 1 Macro-level Mission Architecture. Created by Ashley Loftis.

Once the launch vehicle reaches the desired orbit, the spacecraft is deployed. The propulsion system on the host spacecraft, the BCT X-Sat Venus Class Bus, is used to rendezvous and orient with the selected debris. The debris used for this demonstration is the Electron Kick Stage R/B (ID #60420).

After orientation with the debris is confirmed with the ground station, the capture stage of the mission is initiated. The capture stage of the mission demonstrates two operations: autonomous soft-capture and autonomous hard-capture. Soft-capture is performed by two robotic arms by deploying with the payload and using gecko gripper end-effectors to capture the debris. Once soft-capture is confirmed with ground station, hard-capture is initiated. Hard-capture is performed using the robotic arms to move the predetermined section of the debris into a multi-pin pressure sensor chamber. In the chamber, pins are deployed to mold around the debris. After hard-capture is confirmed with the ground station, the robotic arm end-effectors are removed from the debris, the robotic arms are stored inside the payload, and the capture stage of the mission is complete.

The spacecraft maneuvers to the predetermined orbit, and after confirmation with a ground station, the release stage of the mission is initiated. The release stage of the mission includes one operation, autonomous release. The robotic arms are deployed, and the gecko gripper end-effectors are reattached to the debris. Once the attachment is confirmed with a ground station, the multi-pin pressure sensor chamber is unlocked, and the debris is removed from the hard-capture system. After the removal is confirmed with the ground station, the robotic arm end-effectors are removed from the debris and the robotic arms are stored inside the payload. The release stage of the mission is confirmed, and then the spacecraft deorbits.

By employing gecko grippers as end-effectors, the system can capture a broader variety of debris compared to magnetic end-effectors, which are limited to ferromagnetic materials. Likewise, integrating a multi-pin pressure sensor chamber that conforms to each debris shape enables the secure capture of irregularly shaped objects, expanding the range of debris this payload can effectively handle. Damaging the debris has the potential to create more debris, so the combination of the gecko grippers and the multi-pin pressure sensor chamber as the soft and hard capture mechanisms allow for a gentle approach to capturing and releasing debris.

3 Payload Design

The concept of the design contains three main parts: two robotic arms, gecko gripper end-effectors, and a multi-pin pressure sensor chamber. These three parts work together to perform three autonomous operations—soft-capture, hard-capture, and release—to demonstrate debris removal. The robotic arms are completely foldable and storable inside of the primary structure of the payload, and they both have four joints. The first joint, the “shoulder”, is attached inside a shallow compartment of the payload with a pin. The next two joints are also pins. The last joint, attached to the end-effector, is a rotating (360 degrees) joint. The end-effectors are a gecko gripper material to allow for easy attachment and detachment without damaging the debris [6]. The multi-pin pressure sensor chamber deploys multiple rows of pins to mold around the debris. The tips of the pins also have gecko gripper material to ensure hard-capture. This design can be seen in Figure 2 along with the dimension of each part.

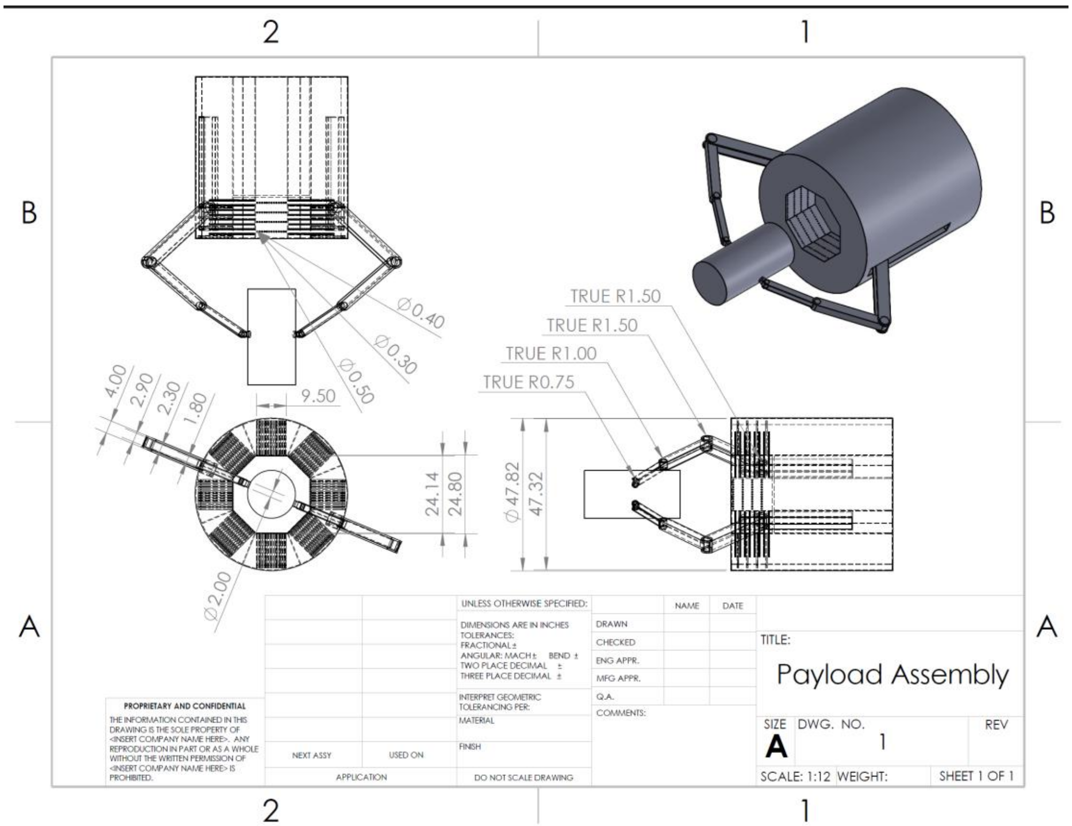

Figure 2 Payload Assembly. Created by Brandon Gero.

The payload performs autonomous soft-capture, autonomous hard-capture, and autonomous release operations to demonstrate debris removal. These operations begin after the spacecraft is oriented with the chosen debris. Autonomous soft-capture begins when the robotic arms are deployed from storage inside of the payload and move to make contact at a predetermined point on the debris. The end effectors are attached at 0 degrees, so the closest segment of the arm is tangent to the surface of the debris. This allows for a consistent and even load to be applied to the debris. Autonomous hard-capture begins when the arms then move a segment of the debris into the multi-pin pressure sensor chamber. The pins are deployed and molded around the debris at various angles. There is a pressure sensor at the bottom of each pin, so once the pin makes contact with the debris, the pressure sensor detects a small load and a command is sent to the pin to stop deploying. At the tip of each pin there is a piece of gecko gripper material to fortify hard-capture. After the pins stop deploying, the end-effectors are detached from the debris by rotating joint so the gecko grippers twist [6]. The arms are then stored inside of the payload and the spacecraft maneuvers to the desired orbit. Autonomous release begins when the robotic arms are deployed and reattached to the debris in the same manner as soft-capture. The pins easily detach from the debris by rotating in a similar manner as the robotic arm end-effectors. The pins will then retract away from the debris, and the robotic arms pull the debris out of the chamber. Once the debris is fully removed from the multi-pin pressure sensor chamber, the robotic arms release the debris by detaching the end-effectors in the same manner as when they are removed after hard-capture. After releasing the debris, the robotic arms are stored inside of the payload. These operations can be found in Figure 3.

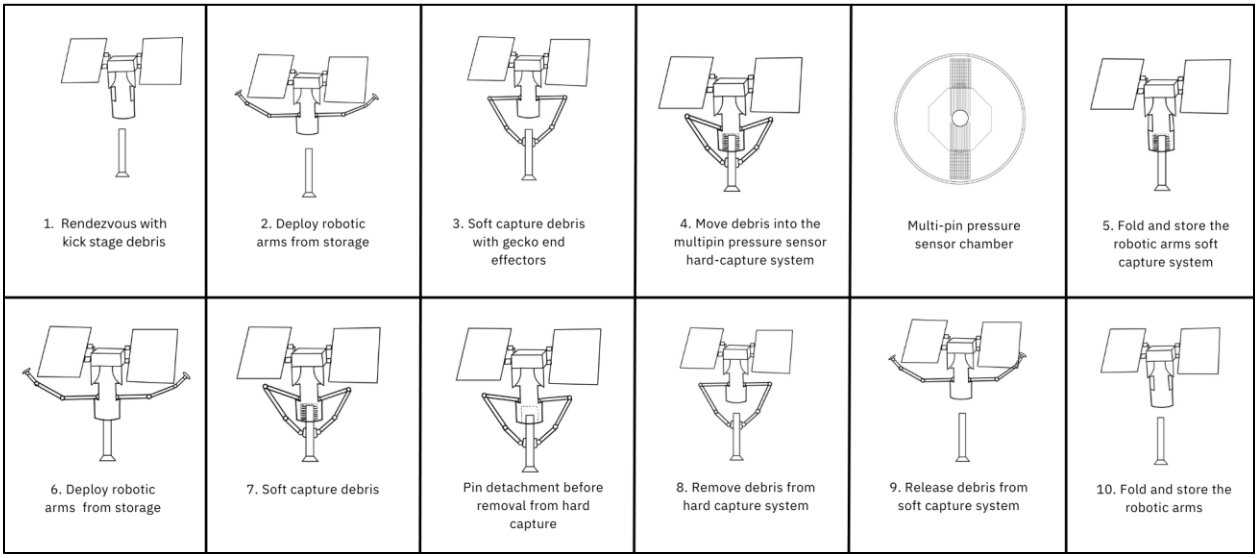

Figure 3 Micro-level Mission Architecture. Created by Ashley Loftis.

Once the mission operations were determined, the payload design was broken down into four subsystems: Optical Tracking, Structure, Thermal, and Command and Data Handling (C&DH). The requirements for each subsystem were determined through the top-level requirements, mission operations, and the assumption that all needed research for materials and systems is available for use. From the four payload subsystems, the needed payload mass was determined to be 21.745 kg or 31.08% of the final mass.

3.1 Optical Tracking Subsystem

The optical tracking subsystem was selected to provide accurate tracking and relative velocity and orientation determination of the target debris during approach and capture operations. Research was conducted to find systems that would be able to track the position and orientation of another spacecraft with precision to enable the spacecraft to safely rendezvous and capture the target debris. Obruta Space Systems’s Rendezvous, Proximity Operations, and Docking Kit (RPOD Kit) was found to meet the requirements and fit in the scale of the spacecraft. The RPOD Kit uses 2 narrow field of view cameras, 2 wide field of view cameras, a floodlight, and onboard processing and storage to determine the relative position of a target within 1% [8]. If loaded with a model of the debris, the RPOD Kit would be capable of determining the relative orientation of the target. This meets the required accuracy of 2.5%.

The RPOD Kit will be mounted near the front of the payload to enable line of sight with the target debris. The system will communicate with bus GNC system to ensure accurate estimations of relative position, orientation, velocity, and rotation. The RPOD Kit is also capable of functioning as a start tracker in the event of partial failure of the GNC system.

3.2 Structure Subsystem

The payload's structure was designed to meet the payload structure subsystem requirements. After developing requirements, an initial configuration of the payload structure was developed. The model includes two robotic arms with end-effectors and a multi-pin pressure sensor chamber. Additional research was done on the gecko gripper material. It was found that gecko gripper material detaches by twisting and allowing the individual setae to detach from the surface at an angle [9]. The primary structure of the payload is modeled as a hollow cylinder. The available volume dimensions for the dual solar-array BCT X-Sat Venus Class Bus given in the RFP, 17.0" x 16.4" x 27", were used to determine the dimensions for the initial configuration. The given volume of 123,276.1cm^3 and a height of 50.8cm were used with the equation for the volume of a cylinder to calculate the outer radius of the structure. The outer radius was calculated to be 23.91cm. Research on payload primary structures was done and showed that a typical payload primary structure thickness was around 0.25cm, so the inner radius of the payload's primary structure was set to 23.66cm to do an initial analysis of structural load conditions.

A trade study was conducted to determine the material of the primary structure of the payload. The criteria used were strength, stiffness, density, thermal conductivity, thermal expansion, specific heat capacity, corrosion resistance, cost, ductility, fracture toughness, ease of fabrication, versatility of attachment options, availability, and launch load conditions. These criteria were used to ensure that the primary structure was able to withstand launch loads while minimizing mass and considering other factors like the space environment and cost. It is important to ensure that the payload can withstand launch load conditions because they are the maximum loads the payload will experience throughout the mission. It is important to minimize mass to ensure fuel efficiency and optimize the limited payload mass of 70kg. The three materials included in the trade study were aluminum 6061, carbon fiber reinforced polymer (CFRP), and titanium [10]. The densities used are 2.72 $\frac{g}{cm^3}$ for aluminum 6061, 0.2$\frac{g}{cm^3}$ for CFRP, and 4.5$\frac{g}{cm^3}$ for titanium [11]. The moduli of elasticities are 68.9GPa aluminum, 95.5GPa for CFRP, and 116GPa for titanium [12]. The moment of inertia in the x and y planes was calculated to be 0.0017m^4 and the axial moment of inertia was calculated to be 0.0034m^4. The payload fundamental frequency was calculated with all three materials using a cantilevered beam assumption and the initial dimensions. The lateral fundamental frequency with Aluminum 6061 was 5.19Hz. With CFRP the lateral fundamental frequency was 22.5Hz, and with titanium it was 5.24Hz. All the frequencies were above the maximum lateral launch frequency of 5Hz with a FOS above 5%. The axial fundamental frequency with Aluminum 6061 was 7.35Hz. With CFRP the axial fundamental frequency was 31.9Hz, and with titanium it was 7.41Hz. All the frequencies were above the maximum axial launch frequency of 5Hz with a FOS above 5%. The trade study, as seen in Table 3, found that aluminum 6061 was best fit for the primary structure of the payload.

Table 3 Payload Structure Material Trade Study

Weight %	Criteria	Aluminum	CFRP	Titanium	1	2	3
14	Strength	3	3	3	Low	Medium	High
12	Stiffness	2	3	3	Low	Medium	High
14	Density	3	3	2	High	Medium	Low
6	Thermal conductivity	3	1	2	Low	Medium	High
5	Thermal expansion	3	3	3	High	Medium	Low
3	Thermal properties (spec. heat cap.)	3	2	2	Low	Medium	High
7	Corrosion resistance	3	3	3	Low	Medium	High
6	Cost	2	1	1	High	Medium	Low
4	Ductility	2	1	2	Low	Medium	High
6	Fracture toughness	2	1	3	Low	Medium	High
3	Ease of fabrication	3	2	2	Low	Medium	High
1	Versatility of attachment options	3	2	3	Low	Medium	HIgh
4	Availability	3	3	3	Low	Medium	High
15	Launch Load Conditions	2	3	2	Low	Medium	High
100	Total	2.57	2.49	2.43			

Since the structural requirements for the payload were verified with the initial estimated dimensions, the dimensions were not changed for the CAD. The Falcon 9 reports that a payload may experience loads up to 6g, so using aluminum 6061 as the material, the estimated critical load for the payload, with a FOS of 10%, is 39.2N [13].

3.3 Thermal Subsystem

The thermal subsystem for the payload was designed to meet the payload thermal requirements and top-level mission requirements. Research was conducted to find the maximum and minimum temperatures for all materials and systems that are being used. It was found that the internal temperature needs to be kept within $-19℃$ to $40℃$ to ensure material and system functionality with a FOS of 1.5. The materials and systems that will be external to the payload all have functionality well outside of the predicted temperatures the payload will experience in LEO; $-65℃$ to $150℃$ [14]. To calculate the radiative heat transfer the payload experiences from the sun, a heat transfer analysis was done in MATLAB using the payload size and orbit information. It was then found that the radiative heat transfer from the sun is $20.68℃$.

To remain within the internal functional temperature range, it was determined that a silicon rubber heater and louvers will be included in the payload thermal system. The louvers were designed to be 50% effective at dissipating heat. This thermal system will be largely used in partial heritage with the Tempco silicon heater, with full heritage being used for the manufacturer and referenced mission. This heater was used in the COMPASS-1 CubeSat developed by the Aachen University of Applied Science and was spaceflight-proven in a Geosynchronous orbit from April 28, 2008 – March 2, 2012 [15]. Small design modifications will need to be made to fit the heater to the LEO environment, including a decrease in size and mass. The size of the heater was reduced to 128.8 in^2 with a mass of $0.175\ kg$.

The Tempco silicon heater will be attached to the top of the payload using pressure sensitive adhesive (PSA) and will be able to raise the internal payload temperature a maximum of $20\ \frac{℃}{min}$ using a watt density of $0.5\ \frac{W}{in^2}$ [16]. The silicon rubber heater will use two thermistors to automatically turn on and off when temperatures extend out of $-14℃$ to $35℃$. A trade study was conducted to determine which thermistor would best fit the mission's needs. The criterion and weights were determined through the heater use requirements [16], resulting in three assessment criteria; Resistance provided, Minimum functional temperature, and Reliability. From this study it was determined that the Gold Chip Thermistor from TE Connectivity [17] will be used in the payload design because it has high reliability, low resistance, and an adequate minimum temperature.

3.4 Command & Data Handling (C&DH) Subsystem

The C&DH subsystem for the payload was designed to meet the payload C&DH requirements. This subsystem will utilize a centralized architecture and will interface to each of the payload's subsystems. This includes the RPOD kit of the orbital tracking system, the robotic arms and end effectors of the structures subsystem, and the sensors, heaters, and thermistors of the thermal subsystem. It is also interfaced with the C&DH system of the bus. Estimates for the weight, size, and power of the C&DH system were completed using information from the SMAD textbook [1] and the overall needed complexity of the system. From this analysis, the size estimate for the C&DH subsystem was 8000 cm^3 with a weight of 5 kg. Additionally, the data volume for the C&DH subsystem was estimated based on the needs of the other subsystems [18]. The data volume estimates for the payload are shown in Table 4.

Table 4 Data Volume Estimates for Payload

Function	Size (Bits)
Optical Tracking (RPOD)	245800
Thermal Control	24600
Robotic Arms	8200
Autonomy	164000
Total	442600

Due to the required autonomy of the mission, a high storage volume is needed to ensure the payload can conduct its needed operations without constant communication with the ground. These data volume estimates will be used to estimate data rates as part of future work to be completed. Additionally, a commercially available computer was selected for the system. The SWRI SC-1750A has been proven on multiple past space missions such as New Millenium DS-1 [1]. However, further research is required to determine if there is full heritage or partial heritage based on what needs to be modified, if anything, to meet mission requirements.

4 Host Spacecraft Integration & Mission Analysis

To ensure mission success, mission analysis and the host spacecraft were also broken down into systems and subsystems. A Launch Vehicle, Orbital Analysis, and Ground Station system were developed for mission analysis and the BCT X-Sat Venus Class Bus was broken down into seven subsystems: Communication, Thermal, Structure, Guidance, Control, & Navigation (GNC), Command & Data Handling (CDH), Propulsion, and Power. Including the subsystems that needed to be added to the bus, the bus mass was determined to be 48.225 kg or 68.92% of the total mass, causing the total mass to be 69.97 kg with 7 kg or 10% of reserve mass allocated to the bus and payload.

4.1 Launch Vehicle

A trade study was completed to determine which Launch Vehicle would best fit the mission's needs. The criterion and weights were determined through the Launch Vehicle requirements, resulting in four assessment criteria: Vibrational Displacement, Payload Fairing Diameter, Reliability, and Cost/kg. The imparted vibrational displacement was calculated for each vehicle by using the Launch Vehicle's user's guide[20][22][24] to find the launch acceleration and frequency that causes the maximum displacement. Table 5 displays the results and weighting for each criterion and prospective Launch Vehicle.

Table 5 Launch Vehicle Trade Study

Criteria			**Launch Vehicle**		
Requirement	**Weight**	**Goal**	SpaceX Falcon 9 [19][20]	Northrop Grumman Antares [21][22]	Northrop Grumman Pegasus [23][24]
Vibrational Displacement	35%	Min	4.97 mm	4.97 mm	0.175 mm
		Normalized	0	0	1
Payload Diameter	35%	Max	3.7 m	3.9 m	1.27 m
		Normalized	0.927	1	0
Reliability	15%	Max	99.34%	94.44%	89%
		Normalized	1	0.526	0
Cost/kg	15%	Min	$2720	$1340	$126410
		Normalized	0.989	1	0
Total			2.913	2.526	1

As shown, the SpaceX Falcon 9 Rocket was selected because it imparts a low Vibrational Displacement, meets Payload Fairing Diameter, has the best Reliability, and a low Cost/kg. It can also be launched out of Cape Canaveral, FL which meets orbit requirements.

4.2 Orbital Analysis

As the mission is centered around capturing and releasing a specific piece of debris, the orbital analysis was driven largely by the particular piece of debris selected. In addition to the constraints, the selection of the piece of debris was influenced by the cost of launching into a similar orbit and the general accessibility of that orbit by ground stations. The Rocket Lab Electron Kick Stage, NORAD ID: 60420 was selected. Details on the debris' orbit are found in Table 6. As most of the mission is centered around the debris' orbit, this was used to conduct initial analysis for other spacecraft systems.

Table 6 Orbital Information of R/B 60420 [25]

Element	Value
Apogee Altitude [km]	609.8
Perigee Altitude [km]	582
Semi-Major Axis [km]	6979
Eccentricity	0.00127
Inclination [deg]	53
Right Ascension of the Ascending Node [deg]	262.1
Argument of Periapsis [deg]	176.8
Orbital Period [mins]	96.71

To assess fuel requirements, the initial orbit after launch was assumed to be a 550km orbit in the same plain as the target orbit, and the target orbit was selected as a coplanar 510km orbit. This latter orbit is the orbit the spacecraft will move the debris to after capture, and where the debris will be released. This orbit was selected for the purpose of demonstrating the payload's ability to retain debris during orbital maneuver and the capability to move debris in general to a designated orbit. The delta V requirements of the rendezvous maneuver was found to be 77 m/s, and the transfer to the target orbit was found to require 150 m/s [26]. Combined, this requires 227 m/s of delta V which leaves 221 m/s for rendezvous and proximity operations related to the capture of the debris, and deorbiting the spacecraft after the mission is accomplished.

4.3 Communication Subsystem and Ground Station

A trade study was conducted to determine which ground system would better suit our needs. The criteria that were used were: Antenna gain-to-noise-temperature, bandwidth, coverage, and the number of locations the company could provide. While our mission will be autonomous and likely not require constant communication, in the case of autonomous failure and manual override is necessary, the criteria selected will be beneficial. These criteria were selected the team wanted a good enough G/T so that the signal can still be received through whatever noise may be present in the system. Similarly, having a good enough bandwidth is beneficial, so that the team can transmit and receive as much data as possible when passes occur. Coverage is a very important characteristic if the autonomy fails. The coverage was based off our selected debris' orbit, and all the ground system options were placed into STK and produced a report on the contact times with respect to the debris, and thus, the larger amount of total contact time, the better. Finally, the number of locations, which isn't as important as coverage because they cover similar bases, however, for the future use of our payload and rendezvous with a different debris, having more locations may be useful [27].

The ground system companies that were selected were Leaf Space, Amazon Web Services, and Atlas Space Operations. Using defined goals for each criterion, maximizing or minimizing, the quantitative decision matrix method was used to determine which option was the best.
With the results from the trade study, it was determined that Leaf Space would be the best option for our mission, and thus more specific research could be done into which locations we would choose and why.

Using STK, all the options for ground stations were input, and the debris the team selected was placed into its orbit. Using the contact time report that's available in STK, three ground stations that were decently spread out across the globe, La Paz, Mexico, Plana, Bulgaria, and Jeju, South Korea, were selected. A data sheet was then provided by the company themselves, and information such as antenna diameter, beamwidth, max antenna input power, and G/T were extracted for each location [28].

Research was done to find options for antenna that the bus possessed, and a data sheet was found for patch antenna's that BCT offers on their buses. To conserve mass and size, the S-band PCB Patch Antenna was selected, which has a beamwidth of about 43 degrees. Link budgets were then able to be made to determine the link margins for the uplink and downlink for each ground station location, as well as the amount of power the communications subsystem would need to use to be successful. For all the link budgets it was determined that the bus will use 2.5 Watts for receiving and 30 Watts for transmitting. It is also expected that the link margins will fall in the range of 5-20 dB, which demonstrates a decent margin of error for communications. The La Paz, Mexico ground station location, which features an antenna diameter of 3.7 m, uplink from and downlink to the bus, provide a link margin of 8.02 dB and 8.13 dB respectively. This confirms our expected values and that given any unexpected noise occurs, communication between the bus and the ground station should still be successful. At the Plana, Bulgaria location, which features an antenna diameter of 4.5 m, the uplink from and downlink to the bus, provide link margins of 10.03 dB and 15.91 dB respectively. Similarly, this shows that if any issues occur or there is more noise interference than expected, there is still a margin where communication can still occur. Lastly, at the Jeju, South Korea location, which features an antenna diameter of 3.9 m, the ground station uplink from and downlink to the bus, provide a link margin of 8.98 dB and 7.96 dB respectively. Like the other two ground stations, the margins provide an error margin where communication will still be possible through any issues [29].

The communication system will be important for the mission as the system on the bus will receive and transmit RF signals to and from the ground stations, and vice versa with the ground station to and from the bus. These RF signals will be sent to a transceiver in the Command and Data Handling portion of the bus that will convert the signals to actual data (ie. Commands). Similarly, the transceiver would also convert data (ie. TT&C information) into RF signals, for the patch antenna to be sent to the ground station. Leaf Space provides SOCC, POCC, and MCC services through their cloud network, which includes TT&C, payload data transmission, and remote MCC. With this, the team won't need to worry about other control centers because everything can be done through their API [30].

4.4 Thermal Subsystem

The thermal subsystem for the host spacecraft was designed to meet the spacecraft thermal requirements and top-level mission requirements. Research was conducted to find the maximum and minimum temperatures for the systems being implemented on the bus. Like the payload, it was found that the internal temperature needs to be kept within $-19℃$ to $40℃$ to ensure material and system functionality with a FOS of 1.5. To calculate the radiative heat transfer the payload experiences from the sun, another heat transfer analysis was done in MATLAB using the bus size and orbit information. It was then found that the radiative heat transfer from the sun is $3.46℃$. The Tempco silicon heater used in the payload will also be used to keep the bus's internal temperature in the optimal range and two of the TE Connectivity Gold Chip Thermistors [17] will also be used to ensure internal bus temperature.

4.5 Structure Subsystem

The BCT X-Sat Venus Class Bus structure was designed to meet the bus structure subsystem requirements. The following subsystems are within the primary structure of the Bus to optimize payload volume for soft and hard capture mechanisms: GNC, C&DH, Propulsion, and Power. The material trade study done for the payload structure subsystem was repeated for the Bus structure subsystem [10-12]. All criteria was weighted and rated the same as the payload except for launch load conditions. Estimated dimensions of 50cm x 50cm x 35cm, a wall thickness of 0.25cm, and the moment of inertia along the y-axis were used to calculate the fundamental frequencies of the Bus structure for each material. The moment of inertia in the x and y planes was calculated to be 4.7E-05m^4 and the axial moment of inertia was calculated to be 8.0E-05m^4. The payload fundamental frequency was calculated with all three materials using a cantilevered beam assumption and the initial dimensions. The lateral fundamental frequency with Aluminum 6061 was 14.0Hz. With CFRP the lateral fundamental frequency was 60.6Hz, and with titanium it was 5.24Hz. All the frequencies were above the maximum lateral launch frequency of 14.0Hz with a FOS above 5%. The axial fundamental frequency with Aluminum 6061 was 18.3Hz. With CFRP the lateral fundamental frequency was 79.4Hz, and with titanium it was 18.4Hz. All the frequencies were above the maximum axial launch frequency of 5Hz with a FOS above 5%. The trade study, as seen in Table 2, found that aluminum 6061 was the best fit for the primary structure of the bus [13].

4.6 Guidance, Navigation, & Control (GNC) Subsystem

The bus Guidance, Navigation, & control subsystem (GNC) was designed to efficiently determine the position and orientation of the spacecraft, and provide sufficient control to reorient the spacecraft, and the debris after capture. Various ADCS solutions from BCT were examined as potential GNC solutions for this mission. The XACT-50, XACT-100, and FLEXCORE systems were compared in a trade study and ultimately the FLEXCORE was selected. Particularly, a configuration of the FLEXCORE using 4 RW8 reaction wheels was selected to provide sufficient momentum and torque for the mission. The RW8 wheels offer 8 Nms of momentum and 0.6 Nm or torque. This configuration allowed for a slew rate meeting the 0.5 deg/s minimum required without debris, and .1 deg/s with debris captured. The FLEXCORE system uses 2 Nano Star Trackers, a sun tracker, a GPS receiver, and a built-in processor to determine the spacecraft's orientation and outputs this data to the reaction wheels, as well as torque rods to maintain orientation and make attitude adjustments. The FLEXCORE has a pointing accuracy of ±0.002 deg. The FLEXCORE will be connected via the CDH system to the payload Optical Tracking system to enable coordinated maneuvering in rendezvous, capture, and departure operations. [30]

4.7 Command & Data Handling (C&DH) Subsystem

The C&DH subsystem for the bus was designed to meet the bus C&DH requirements. This subsystem will utilize a centralized architecture and will interface to each of the bus's subsystems. This includes the sensors, heaters, and thermistors of the thermal subsystem, the FLEXCORE ADCS of the GNC subsystem, the communications subsystem, the propulsion subsystem, and the power subsystem. It is also interfaced with the C&DH system of the payload. Estimates for the size and weight are the same as for the payload C&DH system. Data volume estimates for the bus system are shown in Table 7.

Table 7 Data Volume Estimates for Bus

Function	Size (bits)
GNC (includes propulsion)	442400
Power Management	8200
Communications (Command and Telemetry Processing)	106000
Autonomy	164000
Thermal Control	24600
Total	745200

These data volume estimates will be used to estimate data rates as part of future work to be completed. The same type of computer used for the payload will also be used for the bus. Additionally for the bus C&DH subsystem, a transceiver will be used to send and receive signals for the communication system and convert the signals into data to be used as commands. A trade study was completed to select the transceiver which resulted in the SRS-3 transceiver being selected.

4.8 Propulsion Subsystem

The payload's propulsion subsystem was designed to meet the payload structure subsystem requirements. The propulsion subsystem was designed to meet a criterion of safety that would ensure repeatability of our mission. Safety was measured in terms of historical use of said system type along with volatility of propellent used. The less volatile the propellent, and the more previous mission uses the higher the relative safety rating. An efficient specific impulse relative to a lightweight micro satellite (100kg) was studied to determine the type of propulsion system to be used [31-32]. The higher the specific impulse the more efficient the thruster and therefore the longer the distances the mission would be capable of achieving. The final design parameter studied was the average weight of a specific type of propulsion system. The total weight included the propellent and its pressure vessel tank, all thrusters, all fluid control systems, and attitude control systems if applicable. Over the trade study an average weight was implemented based on Orbion Technologie's Thruster configurator for a Hall effect & cold gas Aurora thruster system [33]. The final design came down to the electric propulsion system provided Orbion patent that doubles as a cold gas attitude control system. The Aurora thrusters range from 100W-300W of variable throttled thrust to achieve a thrust range up to 20mN at 1,400s Isp in Hall effect mode. In cold gas mode the Aurora thrusters reach a thrust of 2N at 30s Isp. The propellent of choice will be compressed Xenon, as it serves dual purpose fueling the Hall effect and cold gas mode thrusters. With a total of 6 thrusters, 4 built into the X-Sat Bus and 2 added onto the payload, this will achieve the total attitude control requirements to match debris object orientation for safe capture. Depending on future mission requirements, room for more propellent may be stored to achieve more reusability. For the current mission, only 5kg of Xenon propellant is worked into the system weight, enough for one mission at a required delta v of $448.2\ \frac{m}{s}$.

4.9 Power Subsystem

The payload's power subsystem was designed to meet the payload structure subsystem requirements. Batteries chosen to comply within mission requirements will be provided by Blue Canyon Technologies. An additional six 2P8S batteries will be on payload along with the three 1P8S batteries the Venus class micro-satellite comes equipped with. The total capacity on board will be 1188Wh/40.8Ah, capable of providing max thrust for approximately one hour total. This estimation is based on the power budget in Table 2 where only four out of the six thrusters will be active at the same time. Analysis of solar panels is based on mission requirements to be capable of continuous operation. The found required solar panel area based on an efficiency of 30% from provided BCT solar panels [30] is $1.435\ m^2$.

5 Risks & Fault Recovery/De-Scope Options

There were six possible risks determined, as shown in Table 8, with the pre-mitigation and mitigation strategy to remedy each risk. Figure 4 displays how effective each mitigation strategy would be at reducing the risk.

Table 8 Risk Mitigation Strategy

Risks	Pre-Mitigation	Mitigation Strategy
1. Launch Window Miss	• Launch Window from Cape Canaveral, FL on [TBD] • Next Window on [TBD]	• Wait until next window • Determine new launch site
2. Gecko Gripper Technology Delay	• Current Technology Readiness Level of 6	• Switch to Magnet end-effectors
3. Pin Pressurization Failure	• Each Pin is individually pressurized	• If in Hard-Capture: death code programmed to override pressure sensor failure • If out of Hard-Capture: cancellation of Release Stage
4. Initial Rendezvous with Debris Miss	• Pre-launch calculations to complete initial rendezvous	• Enough fuel on-board to make 1 maneuver to realign
5. Cause Damage to Debris	• Precise attitude adjustment system to avoid damage	• Reevaluate to determine if mission can be continued or if total mission failure
6. Autonomy Failure	• Potential for autonomy to fail during Capture and Release Stages	• Continuous communication with Ground System for Manual Override

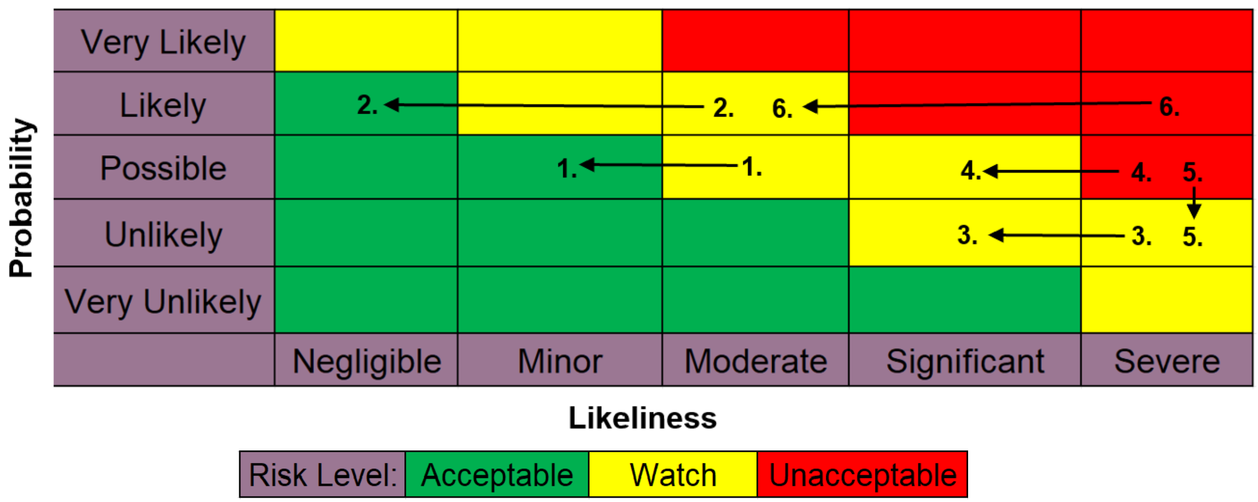

Figure 4 Risk Matrix

Risks 1, 3, and 6 have been pre-mitigated effectively and are unlikely to significantly impact mission success. However, if risks 2, 4, or 5 materialize, the mission would require either descope adjustments or termination. If there is a delay in the gecko gripper technology and a magnetic end-effector was instead used, the mission would have to be de-scoped to only capture ferromagnetic debris. If the initial rendezvous is missed, there is enough fuel on board to complete one maneuver to realign and try again, however if the rendezvous is again missed the mission would have to be terminated. Lastly, if damage is caused to the debris during capture, the debris will be immediately released and reevaluated to determine if the mission can continue with a different capture point or if the damage done was too severe, resulting in mission failure.

6 Future Work

Recommended future work includes combining magnets with the gecko gripper end-effectors, gaining more information on the BCT X-Sat Venus Class Bus, and completing a cost analysis of the design. By exploring the combination of magnets and gecko grippers end-effectors removes the risk of a Gecko Gripper Technology delay and ensures the mission can proceed with a magnetic end-effector. By gaining more information and researching the BCT X-Sat Venus Class Bus will allow for verification of payload and bus integration. Lastly, completing a cost analysis allows for the total cost of the design and the prediction of gained profit.

References

[1] Larson, W., and Wertz, J. *Space Mission Analysis and Design.* Microcosm Press, El Segundo, 1999.

[2] Wertz, J., Everett, D., and Puschell J. *Space Mission Engineering: The New SMAD.* Microcosm Press, El Segundo, 2011.

[3] "About Canadarm," Canadian Space Agency, Longueuil, Quebec, March 2021, https://www.asc-csa.gc.ca/eng/canadarm/about.asp. Accessed: October 23, 2024.

[4] Takane E., Tadakuma, K., Yamamoto, T., Konyo, M., and Tadakoro, S., "A mechanical approach to realize reflexive omnidirectional bending motion for pneumatic continuum robots" ROBOMECH Journal, Vol. 3, No. 28, published online 17 Nov. 2016. https://doi.org/10.1186/s40648-016-0067-x Accessed: October 22, 2024.

[5] Beard, E., "The best 3 magnetic end effectors for your industrial robot," Standard Bots, Glenn Cove, New York, October 2024, https://standardbots.com/blog/the-best-3-magneticend-effectors-for-your-industrialrobot#:~:text=A%20magnetic%20end%2Deffector%2C%20also,magnets%20as%20the%2 0gripping%20mechanism. Accessed: October 23, 2024.

[6] Landau, E., "Gecko grippers moving on up," NASA Jet Propulsion Laboratory, Pasadena, California, August 2015, https://www.nasa.gov/missions/station/gecko-grippers-movingon-up/. Accessed: October 23, 2024.

[7] "What sensors are used in automatic doors?," Safetell, Dartford, United Kingdom, July 2023, https://www.safetell.co.uk/insights/what-sensors-are-used-in-automatic-doors/. Accessed: October 24, 2024.

[8] "RPOD Kit," Obruta Space Solutions, Ontario, Canada, https://www.obruta.com/products. Accessed March 14, 2025.

[9] Liu, Yanwei, Hao Wang, Jiangchao Li, Pengyang Li, and Shujuan Li. 2024. "Gecko-Inspired Controllable Adhesive: Structure, Fabrication, and Application" *Biomimetics* 9, no. 3: 149. https://doi.org/10.3390/biomimetics9030149. Accessed March 13, 2025.

[10] The Engineering ToolBox (2008). *Aluminum Alloys - Mechanical Properties*. [online] Available at: https://www.engineeringtoolbox.com/properties-aluminum-pipe-d_1340.html. Accessed March 13, 2025.

[11] “State-of-the-Art of Small Spacecraft Technology,” NASA Rept. February 2025.

[12] Brizuela Valenzuela, Daniela, María de las Nieves González García, and Alfonso Cobo Escamilla. 2021. "Influence of the Modulus of Elasticity of CFRPs on the Compressive Behavior of Confined Test Pieces and on the Flexural Behavior of Short Concrete Beams" *Applied Sciences* 11, no. 2: 491. https://doi.org/10.3390/app11020491. Accessed March 13, 2025.

[13] Lego, S., “S/C Subsystem Lecture: Structures,” The Pennsylvania State University AERSP401A: Spacecraft Capstone Design, FA24, June 14, 2024.

[14] Plante, J. and Lee, B., “Environmental Conditions for Space Flight Hardware – A Survey,” NASA Electronic Parts and Packing (NEPP) Program, 2004.

[15] Czernik, S., “Design of the Thermal Control System for Compass-1,” *Diploma Thesis*, Aachen University of Applied Science, August 2024.

[16] “Flexible Heaters,” Tempco, Wood Dale, IL, https://www.tempco.com/Tempco/Resources/09-Flexible-Resources/KaptonCatalogPages.pdf. Accessed February 7, 2025.

[17] “NTC Thermistors,” TE Connectivity, Galway, Ireland, https://www.te.com/en/plp/ntc-thermistors/YG2AB.html. Accessed February, 13, 2025.

[18] Lego, S., “S/C Subsystem Lecture: Command and Data Handling (CDH),” The Pennsylvania State University AERSP401A: Spacecraft Capstone Design, FA24, June 14, 2024.

[19] “Falcon 9,” SpaceX, Boca Chica, TX, https://www.spacex.com/vehicles/falcon-9/. Accessed February 6, 2025.

[20] Space Exploration Technologies Corp., “Falcon User’s Guide,” SpaceX, Boca Chica, TX, September 2021, https://www.spacex.com/media/falcon-users-guide-2021-09.pdf. Accessed February 6, 2025.

[21] “Antares Rocket,” Northrop Grumman, Falls Church, VA, https://www.northropgrumman.com/space/antares-rocket. Accessed February 6, 2025.

[22] 2020 Northrop Grumman Corporation, “Antares User’s Guide Release 3.1,” Northrop Grumman, Falls Church, VA, September 2020, https://cdn.northropgrumman.com/-/media/Project/Northrop-Grumman/ngc/space/antares/Antares-Users-Guide.pdf. Accessed February 6, 2025.

[23] “Pegasus,” Northrop Grumman, Falls Church, VA, https://www.northropgrumman.com/space/pegasus-rocket. Accessed February 6, 2025.

[24] 2020 Northrop Grumman Corporation, "Pegasus Payload User's Guide Release 8.2," Northrop Grumman, Falls Church, VA, September 2020, https://cdn.northropgrumman.com/-/media/wp-content/uploads/Pegasus-User-Guide-1.pdf?v=1.0.0. Accessed February 6, 2025.

[25] Track ELECTRON KICK STAGE R/B (NORAD ID: 60420) live with Satcat. https://www.satcat.com/sats/60420?ref=search. Accessed: 14 March 2025.

[26] Casanova. M., "Orbit Rendezvous Calculator," MATLAB Central File Exchange https://www.mathworks.com/matlabcentral/fileexchange/80269-orbit-rendezvous-calculator, 2025.

[27] Lego, S., "S/C Subsystem Lecture: Communications," The Pennsylvania State University AERSP401A: Spacecraft Capstone Design, FA24, June 14, 2024.

[28] Lego, S., "S/C Subsystem Lecture: Ground System," The Pennsylvania State University AERSP401A: Spacecraft Capstone Design, FA24, June 14, 2024.

[29] Leaf Space. Network & Deployment Plan 2025, Leaf Space, Mar. 2025.

[30] Blue Canyon Technologies. *Product Catalog*, Blue Canyon Technologies, 2024. Available: https://www.bluecanyontech.com/static/datasheet/BCT-Product-Catalog.pdf. Accessed March 13, 2025.

[31] Ariane Group. (n.d.). *1N, 20N, 400N and heritage thruster chemical monopropellant thruster family*. Ariane Group Orbital Propulsion 2002-2024, www.space-propulsion.com. Accessed February 20, 2025.

[32] Ariane Group. (n.d.). *10N, 200N, 400N chemical bipropellant thruster family.* Ariane Group Orbital Propulsion 2002-2024, www.space-propulsion.com. Accessed February 20, 2025.

[33] Orbion Space Technology. Houghton, MI. *Aurora Hall-effect propulsion system*. 2025. https://orbionspace.com/product/. Accessed Feb. 25, 2025.